

# Phase space mass bound for fermionic dark matter from dwarf spheroidal galaxies

Chiara Di Paolo,<sup>1,\*</sup> Fabrizio Nesti,<sup>2,3,†</sup> and Francesco L. Villante<sup>4,5,‡</sup>

<sup>1</sup>*SISSA/ISAS, Via Bonomea 265, 34136 Trieste, Italy*

<sup>2</sup>*Dipartimento di Fisica, Theoretical section, Università di Trieste, Strada Costiera 11, I-34151 Trieste, Italy*

<sup>3</sup>*Ruder Bošković Institute, Division of Theoretical Physics, Bijenička cesta 54, 10000, Zagreb, Croatia*

<sup>4</sup>*Dipartimento di Scienze Fisiche e Chimiche, Università dell'Aquila, via Vetoio SNC, I-67100, L'Aquila, Italy*

<sup>5</sup>*INFN-LNGS, Via G. Acitelli 22, 67100, Assergi (L'Aquila), Italy*

We reconsider the lower bound on the mass of a fermionic dark matter (DM) candidate resulting from the existence of known small Dwarf Spheroidal galaxies, in the hypothesis that their DM halo is constituted by degenerate fermions, with phase-space density limited by the Pauli exclusion principle. By relaxing the common assumption that the DM halo scale radius is tied to that of the luminous stellar component and by marginalizing on the unknown stellar velocity dispersion anisotropy, we prove that observations lead to rather weak constraints on the DM mass, that could be as low as tens of eV. In this scenario, however, the DM halos would be quite large and massive, so that a bound stems from the requirement that the time of orbital decay due to dynamical friction in the hosting Milky Way DM halo is longer than their lifetime. The smallest and nearest satellites Segue I and Willman I lead to a final lower bound of  $m \gtrsim 100$  eV, still weaker than previous estimates but robust and independent on the model of DM formation and decoupling. We thus show that phase space constraints do not rule out the possibility of sub-keV fermionic DM.

to Giulia D.S.

## I. INTRODUCTION

Dark matter (DM) is believed to be a main actor in cosmology, to constitute the great majority of the mass in the universe and to rule the processes of structure formation. The so-called  $\Lambda$ CDM paradigm, in which one assumes a cold dark matter (CDM) candidate that decouples from the primordial plasma when non-relativistic, successfully reproduces the structure of the cosmos down to scales  $\sim 50$  kpc.

A number of serious challenges to the  $\Lambda$ CDM paradigm have emerged on the scale of individual galaxies and their central structure, see e.g. [1] for a recent review. For instance, collisionless N-body simulations predict that the DM density profile of virialized objects has a negative logarithmic slope towards the center [2–6]. Such a ‘cuspy’ distribution is not well supported by observational data of rotation curves of spiral galaxies, which are better described by halos featuring a constant density core [7]. Moreover, the number of DM subhaloes expected according within  $\Lambda$ CDM is much larger than the observed number of satellite galaxies in the Milky Way [8, 9], even accounting for the many recently discovered faint systems. It is still unclear whether the above problems require major changes to the  $\Lambda$ CDM paradigm. Models have been presented in which shallow DM cores arise naturally in a  $\Lambda$ CDM cosmology as a results of SN feedback or dynamical friction [10–13]. Alternative DM candidates, however, have to be considered with utmost attention.

The hypothesis of warm dark matter (WDM) decoupling from the plasma when mildly relativistic, has been advocated as a solution of the possible CDM issues. WDM introduces a non vanishing free streaming length below which structure formation is suppressed, giving rise to the correct abundance of substructures at small scales [14–16]. Moreover, if we consider a generic fermionic dark matter (FDM) candidate, like the typical massive  $\sim$  keV warm sterile neutrino, the limit on the phase space density provided by the Pauli exclusion principle implies that DM has a minimal velocity dispersion and, thus, resists compression. As a consequence, FDM halos naturally produce a cored density profile whose radius  $R_h$  (for a fixed halo mass  $M_h$ ) is a decreasing function of the mass of  $m$  of the DM candidate, see next section for details.

The possibility to constrain the DM particle mass by determining the DM phase space distribution was first considered in the seminal work of Tremaine and Gunn in 1979 [17]. In the hypothesis of non-dissipative evolution, i.e. conservation of the maximal phase space density, it is possible to set a strong bounds on the DM mass  $m > 300\text{--}700$  eV, see e.g. [18]. These bounds stem from the primordial limit of the DM phase space density, and are not necessarily related to the fermionic nature of dark matter; indeed they apply also if dark matter can be treated as a collisionless gas collapsed via violent relaxation *à la* Lynden-Bell. However, they require the knowledge of the initial DM phase space density (and, thus, of the DM production mechanism) and the assumption that baryonic feedback cannot alter the maximum of the DM distribution function. A more general situation was studied by Gerhard and Spergel [19] that pointed out the importance of constraints by dynamical friction on dSphs in the Milky Way host halo, that as we will show still play the most important role.

\* chiara.dipaolo@sissa.it

† fabrizio.nesti@irb.hr

‡ francesco.villante@aquila.infn.it

Subsequent analyses [20–22] modeled truly fermionic DM cores for instance by using a Thomas-Fermi self-gravitating-gas approach, suggesting that dwarf spheroidal galaxies host degenerate fermionic halos while larger and less dense galaxies behave as non-degenerate classical systems. Present observational data on DSph galaxies were used in [23] to derive bounds of the order of 400 eV. Finally, in a very recent analysis [24] it was claimed that the rotation curves of the eight classical dwarf spheroidal galaxies of the Milky Way are well fitted by assuming DM cores composed by fully degenerate fermions with masses  $m \simeq 200$  eV and allowing for a non vanishing anisotropy of the stellar component.

The observation that kinematic properties of dwarf spheroidal galaxies may be connected, in a relatively simple model, to the elementary properties of the DM candidate is extremely interesting. However, the evidence in favour of degenerate galactic cores is still inconclusive. In the presence of degenerate halos, the masses and radii of the smallest galactic structures should follow the relationship  $M_h \propto R_h^{-3}$  expected for degenerate fermionic systems and univocally determined by the mass  $m$  of the DM candidate. This behaviour in the plane  $(R_h, M_h)$  is presently not observed; on the contrary, the result that the estimated surface densities of diverse kinds of galaxies is approximately constant [25, 26],  $\Sigma_0 \sim M_h/R_h^2 \sim 100 M_\odot/\text{pc}^2$ , can only be supported by non degenerate cores, because this relation lies almost orthogonal to the above degeneracy lines. Still, this argument cannot be used to rule out the fermionic nature of DM because degenerate cores could be present in the smallest galaxies that are too faint to be observed.

In this paper we take a conservative attitude and we determine a robust lower limit on the mass  $m$  of a fermionic DM particle from the properties of the smallest observed galaxies. We consider Willman I [27] and Segue I [28], which are among the smallest structures for which stellar velocity measurements are available, and the “classical” dwarf spheroidal Leo II from which restrictive bounds on  $m$  were obtained in [23, 24]. We determine bounds on the core radius  $R_h$ , mass  $M_h$  or surface density  $\Sigma_0$  of the selected galaxies by performing a fit to the stellar line-of-sight velocity dispersion profile. The theoretical predictions are obtained through a standard Jeans analysis, including the role of the unknown velocity dispersion anisotropy of the stellar component. Moreover, we refrain from assuming that luminous matter traces the DM distribution, unlike many of the recent works, and thus leave as a free parameter the DM core radius.

We show in detail how, unless the anisotropy of stellar component is constrained independently, the observed stellar velocity dispersion profiles lead to very poor constraints on the DM halo, and the possibility of very large  $\sim \text{kpc}$  halos cannot be ruled out. However, such large halos are at odds with their lifetime due to the dynamical friction within the Milky-Way [29]. This provides a further quantitative limit on the DM halo size, allowing us to finally constrain the DM particle mass  $m$ . To fa-

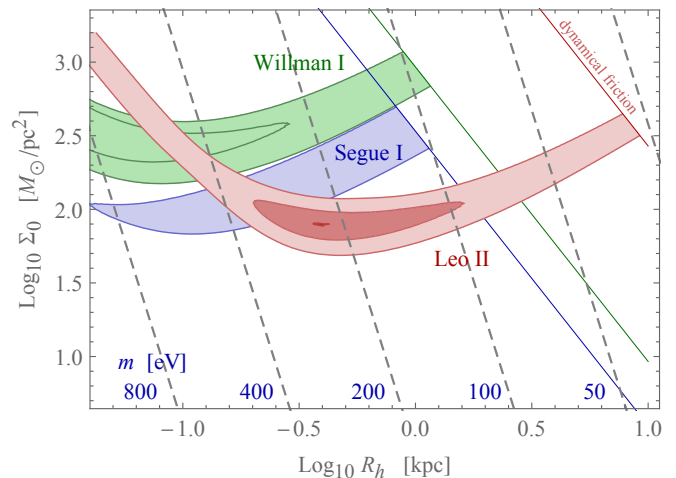


FIG. 1. Plane  $R_h - \Sigma_0$ , describing the DM core. The shaded contours show the values of DM core sizes allowed for Willman I, Segue I and Leo II at 68% C.L. by the LOS velocities, and respecting the bound from the dynamical friction time.

cilitate the reader, our results are anticipated in Fig. 1 that contains a synthesis of our work before discussing the technical details.

The final limit that we obtain,  $m \gtrsim 100$  eV, is less restrictive but more solid than previously quoted bounds [23, 24] which rely on the assumption that the DM core radius is equal to the half-light radius, or analogously that the escape velocity from the DM core is determined by the *stellar* velocity dispersion. Moreover, the limit is fairly model-independent because it is based only on the present phase-space density of DM particles and does not require any assumption on their initial distribution or their evolution (see e.g. [23] for a discussion of the model-dependent bounds that can be obtained for a dissipationless DM candidate by considering specific production mechanisms). Restrictive limits ( $m \gtrsim \text{few keV}$ ) on sterile neutrino mass can be also obtained from the analysis of the Ly- $\alpha$  forest data, see e.g. [30] for a recent update. It should be noted, however, that this analysis is not directly sensitive to DM particle mass; Ly- $\alpha$  data essentially probe the power spectrum of density fluctuations at comoving scales  $\sim \text{Mpc}$ , by constraining the DM free streaming length. Since this quantity can be related to the particle mass only within a specific DM model, the Ly- $\alpha$  bound cannot be applied to a generic fermionic candidate, unlike from the limit derived in this paper.

The plan of the paper is the following: in section II we describe the physics relevant for degenerate fermionic dark matter halos, while in section III we lay down the possible strategies to constrain the mass of the dark matter candidate from the observational data. In section IV we describe the results for the Leo II, Willman I and Segue I dwarf galaxies, by paying also attention to the possibility that some of these galaxies are instead non-degenerate. We present also a consistent estimate for the ensuing bound on the DM mass in the case of the

other known dsph galaxies. In section V we summarize the conclusions and possible outlook. Finally, for convenience we briefly review in the Appendix A the technicalities relative to degenerate fermionic halos, as well as the Thomas-Fermi analysis for non exactly degenerate ones.

## II. THE FDM HYPOTHESIS

We consider the equilibrium configuration for an ensemble of self-gravitating DM fermions of mass  $m$  and  $g$  internal (spin) degrees of freedom. The assumption of fermionic particles implies the upper limit for the DM phase space distribution function that, as reviewed in the appendix A, translates into a lower limit for the DM velocity dispersion

$$\sigma_{\text{DM}}^2 \geq \sigma_{\text{DM,min}}^2(\rho) = \frac{1}{5} \left( \frac{6\pi^2\rho}{g m^4} \right)^{2/3} \quad (1)$$

as a function of the mass density  $\rho$  of the system. This bound becomes effective and very stringent in the regions of high density. As a consequence, fermionic DM halos resist compression and cannot have arbitrary size.

The strong degeneracy limit, in which the velocity dispersion is assumed to have the minimal value  $\sigma_{\text{DM,min}}^2(\rho)$ , represents the most compact configuration for a self-gravitating fermionic halo. The density profiles of such fully degenerate halos are universal. They depend only on one free parameter and can be expressed (apart from a normalization factor and a scale radius which are related, see the following) in terms of the solution of the well-known Lane-Emden equation, see eq. (A13). As shown in the appendix, for our purposes they are very well approximated by the function:

$$\rho(x) = \rho_0 \cos^3 \left[ \frac{25}{88} \pi x \right], \quad x = r/R_h, \quad (2)$$

where  $\rho_0$  is the central DM halo density.

The halo radius  $R_h$  is defined by the condition:

$$\rho(R_h) = \rho_0/4 \quad (3)$$

and is related to the central density  $\rho_0$  and to the properties of the DM particle by the numerical relation

$$R_h = 42.4 \text{ pc} \left( \frac{g}{2} \right)^{-1/3} \left( \frac{m}{1 \text{ keV}} \right)^{-4/3} \left( \frac{\rho_0}{\text{M}_\odot \text{ pc}^{-3}} \right)^{-1/6}. \quad (4)$$

This value represents also the minimal admissible radius for a fermionic structure since for smaller radii the gravitational potential  $\phi \sim -G\rho_0 R_h^2$  is lower (in modulus) than  $\sigma_{\text{DM,min}}^2 \sim (\rho_0/g)^{2/3} m^{-8/3}$  and the system is not stable.

Larger non degenerate structures are admissible because they have  $\sigma_{\text{DM}}^2 \geq \sigma_{\text{DM,min}}^2$  to prevent gravitational collapse. Their properties, however, cannot be univocally predicted because, unlike in the completely degenerate

case, the velocity dispersion is not determined by the mass density and not directly linked to the DM candidate properties. Isothermal halos with arbitrary level of degeneration can be studied by using the Thomas-Fermi approach which is reviewed in the Appendix. Interestingly, it is found that when  $R_h$  is 2–3 times larger than the minimal value (4), the fermionic nature of DM particles can be neglected, i.e. the resulting structures are essentially indistinguishable from isothermal halos obtained by assuming classical Maxwell-Boltzmann statistics and arbitrary large values of the particle mass  $m$ .

For fully degenerate fermionic structures, by using eq. (4) we can predict their surface density  $\Sigma_0 \equiv \rho_0 R_h$

$$\frac{\Sigma_0}{\text{M}_\odot \text{ pc}^{-2}} = 0.584 \left( \frac{g}{2} \right)^{-2} \left( \frac{m}{1 \text{ keV}} \right)^{-8} \left( \frac{R_h}{100 \text{ pc}} \right)^{-5} \quad (5)$$

as well as their mass  $M_h$ , defined as the mass enclosed within the radius  $R_h$ :

$$\frac{M_h}{10^7 \text{ M}_\odot} = 1.18 \left( \frac{g}{2} \right)^{-1/3} \left( \frac{m}{1 \text{ keV}} \right)^{-8} \left( \frac{R_h}{10 \text{ pc}} \right)^{-3}. \quad (6)$$

The radius, surface density and mass of degenerate halos are not independent quantities, being  $M_h \simeq 2.02 \rho_0 R_h^3 = 2.02 \Sigma_0 R_h^2$  for the density profile (2). For definiteness, we perform our analysis in the plane  $(R_h, \Sigma_0)$  but equivalent bounds are clearly obtained by using any couples of the three quantities  $R_h$ ,  $\Sigma_0$  and  $M_h$ .

In Fig. 1 we have reported as gray dashed lines in the plane  $(R_h, \Sigma_0)$  the points relative to fully degenerate systems for selected values of the DM particle mass  $m$  and assuming  $g = 2$ . Eqs. (5) and (6) define the lower limits for surface densities and masses of fermionic DM halos. The regions to the left of the gray lines in the plane  $(R_h, \Sigma_0)$ , are not compatible with the assumption that the halo is composed by fermionic particles. Note that for fixed radius the smaller is the particle mass the larger has to be the surface density. As a consequence, the observational determinations of halo radii  $R_h$  and surface densities  $\Sigma_0$  can be translated into lower limits for the mass  $m$  of fermionic dark matter candidates:

$$\frac{m}{\text{keV}} \geq 0.53 \left( \frac{g}{2} \right)^{-1/4} \left( \frac{\Sigma_0}{100 \text{ M}_\odot \text{ pc}^{-2}} \right)^{-1/8} \left( \frac{R_h}{100 \text{ pc}} \right)^{-5/8} \quad (7)$$

and we note the reduced dependence on  $\Sigma_0$ .

In the presence of degenerate galactic cores, one should arguably observe a clustering of the smallest structures along the lines defined by eq. (5) in the plane  $(R_h, \Sigma_0)$ . This clustering is presently not observed. Instead, the estimated surface densities of diverse kinds of observed galaxies appear to be approximately constant [25, 26],  $\Sigma_0 \sim 100 \text{ M}_\odot/\text{pc}^2$ , a fact that can only be supported by non degenerate cores, because this relation lies almost orthogonal to the degeneracy lines.

This argument cannot be used to rule out the fermionic nature of DM, because even if all large galaxies host a non-degenerate DM halo, degenerate cores could be

present in the smallest objects, clearly of limited number and maybe even too small to be observed. Therefore, what one can do at present is to obtain a lower limit on the mass of a fermionic DM candidate from the existence of smallest galaxies, once their properties (radius, mass and/or surface density) are determined. It is our aim to reassess in this way the present bound on  $m$ .

### III. STRATEGIES

The standard mass estimation methods applied to dwarf spheroidal galaxies, like those described in [31], are not sufficient for our purposes. In fact, they provide an estimator of the mass  $M_{1/2}$  enclosed inside the half-light radius  $R_{1/2}$ , but this radius is not necessarily representative of the DM distribution and may be in principle (much) smaller than the halo size  $R_h$ . In other words, the quantity  $M_{1/2}$  represents only a lower limit on the core mass  $M_h$  but does not provide an upper constraint.

In e.g. [23] and [24], lower bounds on the mass of FDM candidates were obtained by assuming that  $R_h \simeq R_{1/2}$ , i.e.  $M_h \simeq M_{1/2}$  and/or by assuming that the stellar velocity dispersion can be used to estimate the escape velocity from the DM core. This is only allowed if we assume that luminous matter traces DM distribution. However, this assumption may well be violated, especially in the considered scenario in which the properties of the DM distribution are not only determined by gravitational interactions but also by the Fermionic nature of the DM constituents. One may also recall that for larger galaxies, like the Milky Way or elliptical galaxies, the scale lengths of stellar and dark components can differ greatly, with the dark component extending typically some factors more than the stellar one.

Along these arguments, in this work we proceed in more generality, treating  $R_h$  and  $M_h$  as independent properties of the DM halo. We only use  $R_{1/2}$  and  $M_{1/2}$  in a preliminary stage to select, by using the values tabulated in [31] and eq. (6), the dwarf spheroidal galaxies Willman I [27] and Segue I [28] as the most promising candidates for constraining  $m$ . In addition to these two galaxies, which are among the smallest structures for which stellar velocity measurements are available, we also consider the “classical” dwarf spheroidal Leo II from which restrictive bounds on  $m$  were obtained in [23, 24].

For each galaxy, we determine the DM halo properties, core radius and mass (or surface density) by performing a fit of the stellar line-of-sight velocity dispersion profile as predicted by the model through the Jeans analysis, to the observed data. We also consider the role of the possible stellar velocity dispersion anisotropy, and finally we marginalize over it. As was already suggested in the past (see e.g. [32]) in most cases the poor data and more importantly this unknown anisotropy lead to very poor constraints on the DM halo, and the possibility of very large  $\sim \text{kpc}$  halo can not be ruled out. We therefore consider then that such large haloes are at odds with their

lifetime due to the dynamical friction within the Milky-Way, which provides a further quantitative constraint on the DM halo size, and thus allows us to constrain the DM particle mass  $m$ .

#### A. Spherical Jeans analysis

Assuming that the stellar component is virialized within the gravitational potential dominated by the DM component, the standard spherical Jeans equation

$$\left(\frac{\partial}{\partial r} + \frac{2\beta}{r}\right)(n_*\sigma_r^2) = -n_*\frac{GM(r)}{r^2} \quad (8)$$

allows one to relate the velocity dispersion profile of stars to the DM mass distribution  $M(r)$ . In the above,  $G$  is the Newton constant,  $n_*(r)$  is the stellar number density,  $\sigma_r^2$  is the radial velocity dispersion of stars, and  $\beta \equiv 1 - \sigma_\perp^2/\sigma_r^2$  is its anisotropy, which in principle can depend on radius. We first discuss the case of zero anisotropy, and later comment on its role. Our final results are obtained by marginalizing  $\beta$  as a nuisance parameter. A number of other aspects, like the possible coexistence of more than one stellar component, or non-complete virialization, are further factors of uncertainty that may not be easily removed.

The stellar component for each dwarf spheroidal galaxy is quite satisfactorily modeled by means of a Plummer density profile with specific scale radius  $R_*$ :

$$n_*(r) = n_0 (1 + x^2)^{-5/2}, \quad x = r/R_*, \quad (9)$$

and the central density  $n_0$  plays no role in the following.

Eq. (8) can be integrated in favor of  $\sigma_r^2$ , once the dark matter mass distribution  $M(r)$  is determined by the DM density eq. (2). The resulting stellar velocity dispersion is shown in Fig. 2, for three representative cases of  $R_h$  smaller, equal or larger than the stellar scale radius  $R_*$ . The profiles shown are illustrative and are obtained by normalizing to a fixed surface density  $\Sigma_0 = \rho_0 R_h = 1$ . In fact, once the radius  $R_h$  is fixed, the DM central density  $\rho_0$  or the surface density  $\Sigma_0$  represent just a multiplicative constant factor for the mass function  $M(r)$  and do not affect the radial dependence of  $\sigma_r^2$ .

We see from Fig. 2 that if the DM halo is smaller than the Plummer radius,  $R_h \leq R_*$ , the stellar velocity dispersion starts to fall as soon as the DM density vanishes, reflecting the decrease of the gravitational potential. On the other hand if the DM distribution is more extended than the stellar one,  $R_h \geq R_*$ , the stellar velocity dispersion has to increase in the regions where the Plummer density drops. In few words, the slope of the stellar velocity dispersion  $\partial \ln \sigma_r^2 / \partial \ln r$  is related to the characteristic sizes  $R_*$  and  $R_h$  of the galactic components and could, thus, be used to constrain the DM distribution.

In order to compare with observational data, one has also to consider that only the velocity dispersion *along*



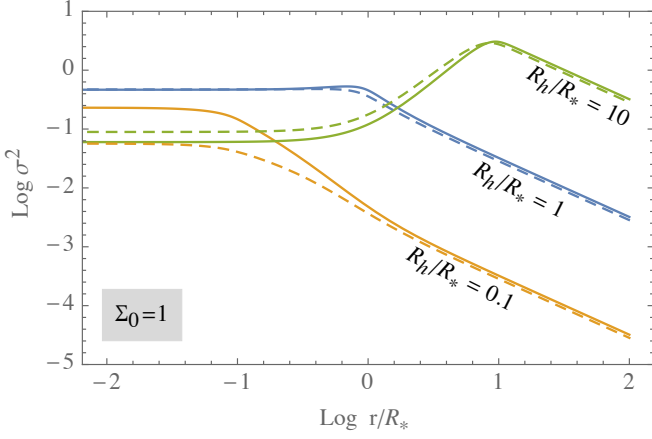


FIG. 2. Stellar velocity dispersion profiles (solid) for representative DM core radii and  $\beta = 0$ . The dashed curves show the line-of-sight projected dispersion velocity profiles.

the line of sight (LOS) is measurable:

$$\sigma_{\text{los}}^2(R) = \frac{1}{\Sigma_*} \int_{R^2}^{\infty} dr^2 \frac{n_*(r)}{\sqrt{r^2 - R^2}} \sigma_r^2 \left[ 1 - \beta \frac{R^2}{r^2} \right], \quad (10)$$

where  $\Sigma_*(R) = \int_{R^2}^{\infty} dr^2 n_*(r)/\sqrt{r^2 - R^2}$  is the projected stellar (surface) density. In Fig. 2, we show with dashed lines the LOS velocity dispersion for the three cases described previously. They retain the same behaviour of  $\sigma_r^2$ , showing that the observed LOS velocity dispersion profile  $\sigma_{\text{los}}^2(R)$  can in principle be used to constrain the size of the DM core.

### B. The role of anisotropy

As is well known and as we will see in detail, the unknown stellar velocity dispersion anisotropy  $\beta$  limits severely the possibility to extract the DM core radius  $R_h$  from observational data. Indeed, in the absence of direct information, the quantity  $\beta$  has to be treated as a nuisance parameter that has to be removed in order to compare a mass model with observations (see e.g. [33] and [34] for a recent critical discussion). The role of  $\beta$  can be understood by rewriting the Jeans equation (8) in the form

$$\frac{\partial \ln \sigma_r^2}{\partial \ln r} = -\frac{1}{\sigma_r^2} \frac{GM}{r} - \gamma_* - 2\beta \quad (11)$$

where  $\gamma_* = d \ln n_*/d \ln r$  is the slope of the stellar number density, that runs from  $\sim 0$  near the center to negative values out of  $R_*$ . Note that the first two terms in the r.h.s. which are related to DM and stellar distributions have opposite signs, being negative the first and positive the second. In the case of zero anisotropy, the slope of the velocity dispersion vanishes at the galactic center, i.e.  $\partial \ln \sigma_r^2 / \partial \ln r = 0$  for  $r = 0$ , since these two terms are both equal to zero in the origin. If the DM halo extends outside the stellar scale radius, the term  $\gamma_*$  starts to grow

(in modulus) at  $r \simeq R_*$  while  $GM(r)/r\sigma_r^2$  is still negligible, and determines the positive slope of  $\sigma_r^2$  observed in Fig. 2. Whereas the observed stellar velocity dispersion does not feature such a growth at large distances, one can set an upper bound on the DM core radius, that can not be much larger than the stellar scale radius  $R_*$ .

The presence of a non vanishing anisotropy can clearly alter this scenario. In particular, a positive  $\beta$  can compensate the effect of  $\gamma_*$  reducing the outer slope of  $\sigma_r^2$ , even in presence of a DM distribution extending well beyond the stellar radius. However, this effect is limited by the fact that the anisotropy parameter is limited to be less than 1. As a result, the case  $\beta = 1$  leads to weaker upper bound on the core radius  $R_h$ , and basically the most conservative. The opposite holds for negative  $\beta$  values that can give quite small slope  $\partial \ln \sigma_r^2 / \partial \ln r \geq 0$  even for mass models with  $R_h \leq R_*$ . Because a negative  $\beta$  is unconstrained, this limits the possibility of setting a lower bound on  $R_h$  in dwarf spheroidals and assessing the cusp-core problem at such short scales.

In our analysis, we assume a *constant* anisotropy parameter  $\beta$  and we extract the DM core radius  $R_h$  and surface density  $\Sigma_0$  (or mass  $M_h$ ) by marginalizing the fit to the observed dispersion velocity profile in the range  $-\infty \leq \beta \leq 1$ . For comparison, Wolf et al. [31] considered  $r$ -dependent profiles parameterized by suitable functions with  $-10 \leq \beta \leq 0.91$ . Note that, for the purpose of determining an upper limit for the core radius  $R_h$ , it is not even necessary to consider a generic  $\beta(r)$  since the most relevant fact is the presence of the upper bound  $\beta < 1$ .

### C. Analysis for the smallest objects

In order to obtain the most restrictive bounds on the mass of the FDM particle, below we will consider Willman I [27] and Segue I [28] which are among the smallest observed galactic structures. The problem with these objects is that the number of stars for which a measure of velocity is available and which pass quality cuts is quite small (i.e. less than 50). As a consequence, it is not possible to determine the velocity dispersion in radial bins sufficiently localized to be compared directly with the profile in eq. (10). One can still appreciate the characteristic signature of a large DM core, i.e. an increasing slope of the stellar dispersion velocity between  $r \sim R_*$  and  $r \sim R_h$ , by determining the velocity dispersion in few relatively large bins with dimension  $\Delta r \sim R_*$ .

In order to perform such analysis, we define the *average* LOS velocity dispersion in a bin  $r \in [R_1, R_2]$ ,

$$\overline{\sigma_{\text{los}}^2}(R_1, R_2) = \frac{1}{N_*(R_1, R_2)} \int_{R_1}^{R_2} dr 2\pi r \Sigma_*(r) \sigma_{\text{los}}^2(r), \quad (12)$$

where  $N_*(R_1, R_2) = \int_{R_1}^{R_2} dr 2\pi r \Sigma_*(r)$  is the cumulative number of stars between two radii. Using (10), and as-

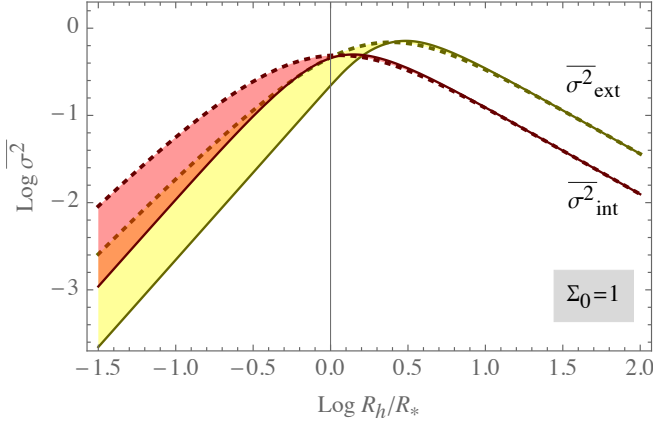


FIG. 3. Averaged stellar velocity dispersion in two bins, taken here as *int* =  $[0, r_*)$  (red) and *ext* =  $[r_*, 3r_*)$  (yellow), for  $\beta = 0$ . The dashed curves show the same for a Burkert profile (nondegenerate fermions).

suming constant  $\beta$ , we find

$$\overline{\sigma_{\text{los}}^2} = \frac{1}{N_*(R_1, R_2)} \int_{R_1}^{\infty} dr 4\pi r^2 n_* \sigma_r^2 \mathcal{F}(r, \beta; R_1, R_2), \quad (13)$$

where the adimensional function  $\mathcal{F}(r, \beta; R_1, R_2)$  is

$$\mathcal{F}(r, \beta; R_1, R_2) = \left\{ \left[ \sqrt{r^2 - R_1^2} - \sqrt{r^2 - B^2} \right] \frac{(3 - 2\beta)}{3r} + \frac{\beta}{3r^3} \left[ B^2 \sqrt{r^2 - B^2} - R_1^2 \sqrt{r^2 - R_1^2} \right] \right\} \quad (14)$$

with  $B = \min\{r, R_2\}$ .<sup>1</sup>

For illustrative purposes, we show in Fig. 3 as solid lines the behaviour of the average LOS velocity dispersion calculated in two bins  $[0, R_*)$  and  $[R_*, 3R_*)$  as a function of the DM core radius  $R_h$ , for  $\beta = 0$ . One can observe that the average LOS dispersion velocity in the external bin overshoots the internal one as soon as  $R_h/R_* \gtrsim 2$ . This demonstrates that even with two single bins, and provided the uncertainties on the observed dispersion velocity are not too large, one could constrain the DM core size. For instance, if the observed dispersion velocities in two or more bins in the vicinity of  $r \simeq R_*$  are approximately constant, one can rule out the possibility that DM extends much beyond the stellar component.

From the plot one can make also other remarks. Clearly, the more the DM core extends beyond the stellar component ( $R_h/R_* > 1$ ) the less its actual density profile beyond  $R_h$  is relevant for the stellar physics, because the DM density is anyway constant in the region where the stars trace the gravitational potential. On the other hand, one can expect that if the DM core is smaller than the stellar scale ( $R_h/R_* < 1$ ) the actual shape of the DM profile out of its core will influence the resulting stellar

velocity dispersion. To show this effect, we have repeated the analysis also for Burkert DM profiles, reported also in Fig. 3 as dashed lines. As one can see, for  $R_h > R_*$  the solid and dashed curves are overlapping, i.e. the predicted dispersion is independent from the shape of the DM profile, which makes the analysis more robust.

Unfortunately, as we shall discuss for the specific cases of Segue I and Wilman I, the analysis outlined in this section is considerably hampered by the large uncertainties in each bin of the observed velocity dispersion. In addition, it is also severely limited when one leaves unconstrained the anisotropy. While one can hope that the accuracy of the observational data will improve, the situation with the anisotropy is more dramatic; it would be necessary to strongly limit  $\beta$  in order to extract useful limits from the observational velocity dispersion data.

#### D. Dynamical friction

The mass of dwarf spheroidals can be limited from above because they are subject to dynamical friction in the Milky-Way DM halo. Their orbit decay with a characteristic time scale that can be estimated from the Chandrasekhar's formula [29]

$$t_{\text{fric}} = \frac{10^{10} \text{ y}}{\ln \Lambda} \left( \frac{D}{60 \text{ kpc}} \right)^2 \left( \frac{v}{220 \text{ km/s}} \right) \left( \frac{2 \cdot 10^{10} M_{\odot}}{M_h} \right) \quad (15)$$

where  $v$  is the velocity of the dwarf galaxy and  $D$  is its distance from the Milky-Way center. The Coulomb logarithm in the above equation is given by

$$\ln \Lambda = \ln \left( \frac{b_{\text{max}}}{b_{\text{min}}} \right), \quad (16)$$

where  $b_{\text{max}}$  and  $b_{\text{min}}$  are the maximum and minimum impact parameters. These can be estimated as [29, 35]:

$$b_{\text{max}} = - \left( \frac{d \ln \rho_{\text{MW}}}{dr} \right)^{-1} \simeq \frac{D}{\gamma} \\ b_{\text{min}} = \max \left\{ R_h, \frac{GM_h}{v_{\text{typ}}^2} \right\} \quad (17)$$

where  $v_{\text{typ}}$  is the virial velocity and we assumed that the Milky Way DM density scales approximately as  $\rho_{\text{MW}} \propto D^{-\gamma}$  with  $\gamma \simeq 2$  in the vicinity of the objects considered.<sup>2</sup>

Chandrasekhar's formula (15) is known to fail when the mass of the mass  $M_h$  of the satellite becomes comparable to the mass of the host system that lies interior to the satellite's orbit and/or the density of host system is constant, see e.g. [36]. In the cases of our interest, however, none of these conditions apply and eq. (15) provides a remarkably accurate description. By requiring

<sup>1</sup> The quantity  $N_*(R_1, R_2)$  can be also calculated as  $N_*(R_1, R_2) = \int_{R_1}^{\infty} dr 4\pi r^2 n_*(r) \mathcal{F}(r, \beta = 0; R_1, R_2)$

<sup>2</sup> For degenerate cores, the halo radius  $R_h$  defined in eq. (A14) is sufficiently close to the half mass radius of the DM distribution.

$t_{\text{fric}} \gtrsim 10^{10} y$ , and by considering that the typical velocity of satellites should be of the order of the Galactic virial velocities at those distances  $\sim 220 \text{ km/s}$  [37], one finds a bound on the mass  $M_h$  that depends on the distance of the dwarf galaxy from the Galactic center.

Note that the existence of an upper limit for  $M_h$  does not imply by itself the possibility to constraints the FDM scenario. Gerhard and Spergel [19] noted, however, that if the DM density of dwarf spheroidal galaxies can be determined from velocity dispersion data, the upper bound on  $M_h$  can be used to obtain an upper limit on  $R_h$ , thus constraining the mass  $m$  of hypothetical FDM particles.

## IV. RESULTS

### A. A small classical Dwarf - Leo II

As a paradigmatic case, we first analyze the case of Leo II, the smallest among the so-called 'classical' dwarf spheroidal satellite galaxies of the MW. The stellar number density of Leo II is well modeled by a Plummer profile with scale length  $R_* = 177 \text{ pc}$ . In Fig. 4 we report the observed stellar LOS velocity dispersion,  $\sigma_i^2 \pm \delta\sigma_i^2$ , measured in 11 bins centered at the radii  $r_i$ . We compare these data with the LOS velocity dispersion predicted in (10) for the fully degenerate fermionic DM halo,  $\overline{\sigma}_i^2 \equiv \sigma_{\text{los}}^2(r_i)$ , by defining a standard  $\chi^2$  test:

$$\chi^2(R_h, \Sigma_0, \beta) = \sum_{i \in \text{bins}} \left( \frac{\sigma_i^2 - \overline{\sigma}_i^2}{\delta\sigma_i^2} \right)^2. \quad (18)$$

The model parameters are the DM core radius  $R_h$  and surface density  $\Sigma_0 \equiv \rho_0 R_h$ , plus the anisotropy  $\beta$ . Note that, as long as we consider a fully degenerate halo, the couple of parameters  $(R_h, \Sigma_0)$  correspond to a well defined value of the mass  $m$  of the FDM candidate according to eq. (5).

Our results are shown in Fig. 5. In the left frame, we plot the  $\chi^2$  contours in the plane  $(R_h, \Sigma_0)$ , corresponding to 68% CL exclusion for 11 degrees of freedom (dof), obtained by assuming fixed values of  $\beta = -0.5, \dots, 1$ . In the right frame, we marginalize the anisotropy parameter, i.e. for assumed values  $R_h$  and  $\Sigma_0$  we choose the optimal  $\beta$  that minimizes the  $\chi^2$ , and plot the contours of this minimal  $\chi^2$ . The light shaded area corresponds to  $\chi^2 = 11.5$  that gives 68% CL exclusion for  $11 - 1 = 10 \text{ dof}$ <sup>3</sup>.

The absolute minimum  $\chi_{\text{min}}^2 \simeq 2.5$  corresponds to a very good fit of the observational data, as can be seen by

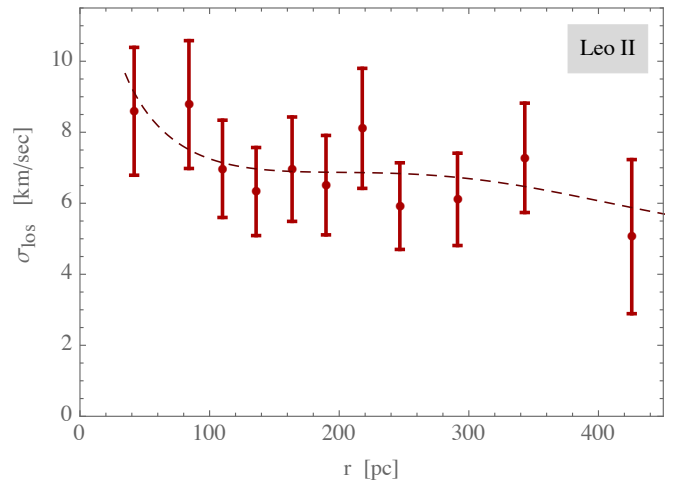


FIG. 4. Stellar line-of-sight velocity dispersions for Leo II. The dashed line represents the best fit, achieved for  $\beta = 0.6$ .

the velocity dispersion profile superimposed on figure 4. This is achieved with  $\beta = 0.6$  and is relative to a core size  $R_h \simeq 400 \text{ pc}$  and surface density  $\Sigma_0 \simeq 75 M_\odot/\text{pc}^2$ . These values correspond to a degenerate fermionic core for a DM mass  $m \simeq 0.23 \text{ keV}$ , in good agreement with the value suggested by [24].

In Fig. 5, we also show with dashed lines the  $(R_h, \Sigma_0)$  values corresponding to degenerate cores for fixed values of the particle mass. For each value of  $m$ , the configurations to the left of the line are forbidden, so that one could obtain a lower bound on the DM particle mass directly from this plot. We see, however, that unless the anisotropy  $\beta$  is constrained independently, velocity dispersion data do not provide an upper bound on the size of the DM halo and thus do not allow to set limits on  $m$ . In particular, for maximal values of  $\beta \sim 1$ , i.e. radial motion of stars, a multi-kpc structure is allowed. This situation is most likely not realistic, being unlikely that such huge DM halo hosts a stellar system of just few hundredth pc and small velocity dispersion. It is however difficult to give at this stage a quantitative support to this observation. Note, indeed, that the  $\chi^2$  becomes flattish for  $R_h \gg R_*$  because the limited extent of the stellar component does not permit to constrain a much larger DM halo.

The above conclusion can be made more quantitative by producing a one-dimensional  $\chi^2$  profile as a function of  $m$ . This is obtained by eliminating the radius  $R_h$  in favour of the mass  $m$  through eq. (5) and then marginalizing with respect to  $\Sigma_0$ . The final result is shown in Fig. 6, as a red curve. We see that no lower limit on the particle mass  $m$  can be obtained, even at 68% CL that would require  $\chi^2 > 10.4$  for a distribution with  $11 - 2 = 9 \text{ dof}$ . We remark that although the  $\chi^2$  increases beyond the minimum at  $m \geq 0.23 \text{ keV}$ , this cannot be used to set an upper bound on  $m$ , unless one assumes that Leo II has a fully degenerate DM halo. The observed  $\chi^2$  behaviour for large masses is indeed related to the fact that the ra-

<sup>3</sup> Since we are interested in a bound on  $m$  by excluding a region of the  $(R_h, \Sigma_0)$  plane (marginalizing  $\beta$ ) we use the absolute  $\chi^2$  to determine the level of compatibility with observational data. If instead one assumes that the FDM hypothesis is correct, the 68% CL allowed region in the plane is determined by  $\Delta\chi^2 \equiv \chi^2 - \chi_{\text{min}}^2 = 2.3$  (for 2 dof). For completeness, we show this region with dark shaded area in Fig. 5

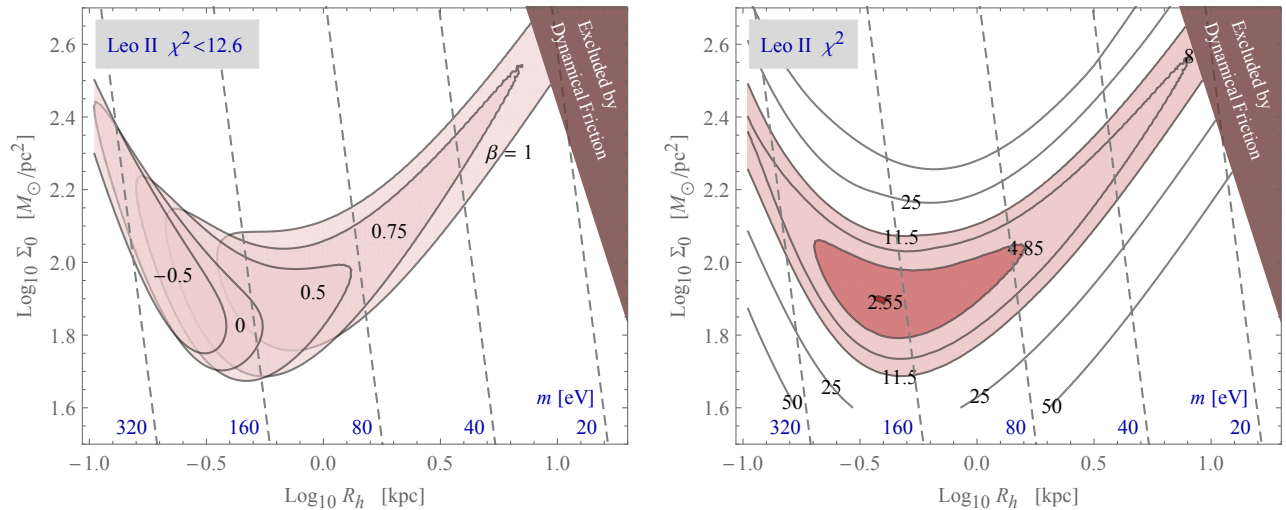


FIG. 5. LEO II – Left: Contours of compatibility with data at 68% probability ( $\chi^2 \lesssim 12.6$ , for 11 dof) as a function of the degenerate DM core parameters, for various values of the dispersion anisotropy  $\beta$ . Right: Contours of best  $\chi^2$  in the plane  $(R_h, \sigma_0)$  after marginalizing the anisotropy  $\beta$ . The light shaded region is compatible with the observational data at 68% CL ( $\chi^2 \lesssim 11.5$ , for 11-1=10 dof). The darker shading shows the region preferred by data at 68% CL ( $\Delta\chi^2 = 2.3$ ), if one assumes the FDM hypothesis as true.

dius of degenerate fermionic cores is too small to provide a good fit to observational data. However, the possibility that the considered galaxy has a non-degenerate halo with a radius  $R_h$  larger than the lower limit allowed by the quantum exclusion principle cannot be excluded.

In order to clarify this point and put this argument to test, we repeat the above analysis by considering a (non-degenerate) cored Burkert profile with radius 2 times larger than the minimal value given by eq. (4). This gives the  $\chi^2(m)$  contour represented by the blue line in figure 6. The assumed profile leads to better fits for large masses while the  $\chi^2$  slowly converges to the degenerate case at the left end of the plot, as it is expected by considering that for small  $m$  the DM core is necessarily much more extended than the stellar component so that the assumed density profile beyond the core has no impact on the observed  $\sigma^2$ . The above test could be repeated by considering other admissible non-degenerate profiles and the overall marginalized  $\chi^2$  should be obtained by determining the minimal value at a fixed mass  $m$ . Since the assumed profile does not play any role for small  $m$  and we expect a smooth transition between the non-degenerate and degenerate case, the final  $\chi^2$  has to be thought as independent from the DM mass (i.e. flat) starting just beyond the minimum of the degenerate case. Indeed, the particle mass  $m$  has to play no role in the nondegenerate regime. This is shown by the continuous red line and by the red shaded region in Fig. 6.

Even if stellar velocity dispersion data, taken alone, do not allow to obtain a limit on  $m$ , the mass of the DM particle can be constrained by considering that the halo decay time due to dynamical friction (15) becomes unacceptably small for very large objects. Indeed, in the limit  $R_h \gg R_*$  the quantity directly constrained by stel-

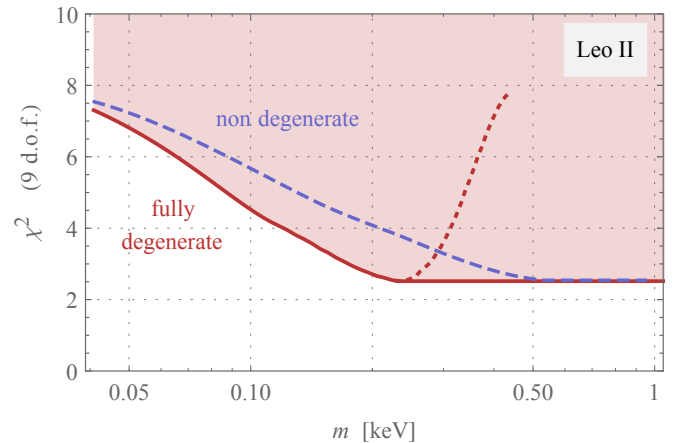


FIG. 6. LeoII - Minimal  $\chi^2$  marginalized over  $\beta$  and one DM halo parameter (along each degeneracy line relative to  $m$ ). The shaded region represents the overall minimal  $\chi^2$  taking also into account the possibility of nondegenerate halos (see text for discussion).

lar velocity dispersion data is the halo central density  $\rho_0 = \Sigma_0/R_h$ . Therefore, by moving along the  $\chi^2$  flat direction at increasingly larger radii in Fig. 5, the halo mass increases as  $R_h^3$  and eventually reaches values  $M_h$  that correspond to unacceptable friction times (15). This constraint is reported on Figs. 5, by cutting the regions where friction times are unphysical.

In conclusion, the interplay between dynamical friction and velocity dispersion data allows us to determine an absolute upper bound on the halo size, and thus a lower bound on the DM mass. For Leo II, this results in a very weak constraint,  $m \gtrsim 25$  eV.



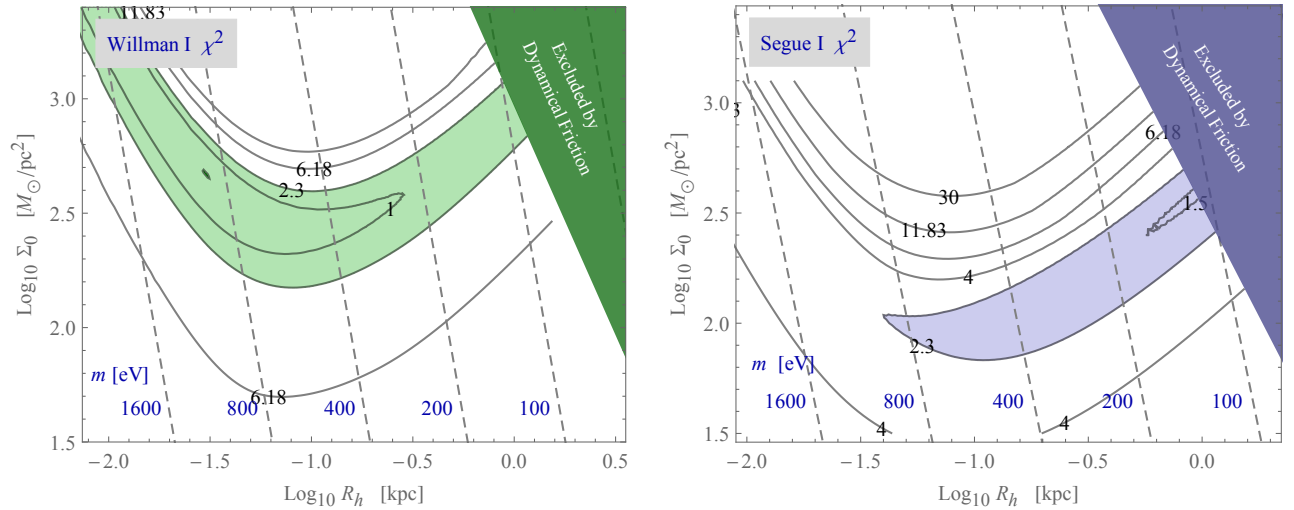


FIG. 7. Contours of  $\chi^2$ , after marginalizing on the free range of  $\beta$ . The left panel is for Willmann I, while the right panel refers to Segue I. The light shaded regions give the region of compatibility with data at 68% CL ( $\chi^2 = 2.3$ , 2 dof). Notice that no upper limit on the confidence interval on the radius can be placed for either galaxy.

### B. Smallest Dwarf spheroidals: Willman I and Segue I

Let us apply the above strategies to the case of the Willman I and Segue I dwarf spheroidal galaxies [27, 28] which are among the smallest galaxies for which line of sight velocities are available. Their stellar distributions are fitted by Plummer profiles with very small radii, given by  $R_* = 25$  pc and  $R_* = 29$  pc, respectively. We use the stellar velocity data to determine the velocity dispersion in three bins with extension comparable to the Plummer radii. The results obtained are reported in Fig. 8 as a function of the projected distance from the galactic center. We compare these observational results with theoretical predictions by defining a standard  $\chi^2$  where in

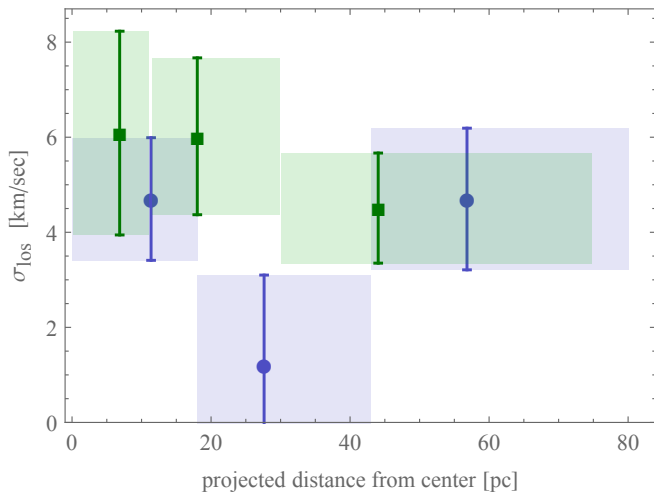


FIG. 8. Line of sight velocity dispersion in Willman I (green squares) and Segue I (blue circles).

each bin we adopt the averaged LOS dispersion, Eq. (13). We repeat the procedure adopted for Leo II, i.e. we minimize the  $\chi^2(R_h, \Sigma_0, \beta)$  in the full range  $-\infty < \beta \leq 1$  of the anisotropy in order to marginalize with respect to it. Our results are reported in figure 7, where we show the  $\chi^2 \equiv 2.3$  contours corresponding to 68% CL exclusion for  $3 - 1 = 2$  dof for Willman I in the left frame and for Segue I in the right frame.

We note that no significant constraints on the halo radius are obtained for Willman I. Indeed, a good fit is achieved for  $R_h \ll R_*$  by allowing the anisotropy  $\beta$  to be increasingly negative. On the other hand, the fit worsens for large core radii but the  $\chi^2$  becomes flattish beyond  $R_h \sim 300$  pc and is not sufficiently large to give a significant exclusion of larger halo sizes. This is clearly due to the limited radial extension of the stellar data sample,  $\sim 75$  pc. The best fit is obtained for  $R_h \simeq 30$  pc,  $\Sigma_0 = 473 M_\odot/\text{pc}^2$  and  $\beta = -0.2$  and corresponds to  $\chi^2 \simeq 0$ , as it is expected by considering that we have only three bins and three free parameters.

Again, even if the DM radius is not constrained, the fits provide a useful determination of the central density of the system, that defines the  $\chi^2$  flat direction in the plane  $(R_h, \Sigma_0)$  for  $R_h \gg R_*$ . Similarly to Leo II, by requiring that the dynamical friction decay time for Willman I is not too small, we can exclude large core radii beyond  $\sim \text{kpc}$  in the upper-right shaded region in 7, and obtain a robust lower bound on the DM mass  $m \gtrsim 80$  eV.

An analogous analysis holds for Segue I, whose binned velocity dispersions are reported with blue circles in Fig. 8. The three bins show that Segue I presents a different profile with respect to other dwarfs, with the velocity dispersion rising beyond  $\sim 40$  pc. This behavior, that has already been noted in the literature as a possible evidence of a large DM halo (or an indication against its regularity/virialization) is consistent with the

expectations from a scenario with  $R_h \gg R_*$ . Consistently, small radii  $R_h \lesssim 40$  pc cannot be accommodated by the fit, even assuming a stellar anisotropy parameter  $\beta \leq 0$ . The best fit is obtained for  $R_h \sim \text{few kpc}$  and no upper limits can be derived from Jeans analysis. Nevertheless, the central halo density is determined and the halo extension is limited again by the constraint on the dynamical friction time, as shown in Fig. 7. The resulting lower bound on the DM mass is slightly better to that derived for Willman I,  $m \gtrsim 100$  eV, mainly due to the fact that Segue I is closer to the galactic center.

### C. Other Dwarfs

As a cross check, we note that the results presented above for the Jeans analysis are indeed compatible with the fits performed in the recent work [38] where the authors also consider the possibility of triaxial halos and arbitrary density profile slope at the center. While their analysis does not consider degenerate fermionic halos, their results confirm that for most dwarf galaxies the DM halo radius is quite poorly constrained, and halos of few kpc size appear to be allowed by the data, even if this is most likely unphysical. For our purposes, as discussed above, what drives the bound on the DM mass is the interplay of the dynamical friction constraint with the central halo density  $\rho_0$ , which is the quantity constrained by observations in the limit of large halo size. Because this central density is largely independent on the (outer) halo shape, we can take advantage of the results of [38] to estimate the DM mass bound for all objects presented in that work. The bound is in fact driven by the central DM density and the distance of the dwarf satellite. As we see, by using the central fitted values of the densities, our result of Segue I and Leo II are confirmed, so that the results given in this work represent the most conservative bound around  $m \gtrsim 100$  eV, with a possibly slightly stringent bound from the Triangulum II galaxy.

## V. DISCUSSION AND CONCLUSIONS

In this work we have reassessed the lower bound on the mass of a fermionic dark matter candidate, independently from particular models of its production or history of its clustering. The quantum nature of such light fermionic candidate implies an upper bound on the phase space density in currently observed objects, and the knowledge of the density can be turned into a lower bound on the mass, *à la* Tremaine-Gunn. We have reconsidered the smallest Dwarf Spheroidal galaxies, that according to kinematical data are believed to host the largest densities of dark matter, thus constituting the ideal candidates to set a lower bound on the DM mass  $m$ .

Such a bound must be set in the hypothesis of DM halo composed by a completely degenerate gas of fermions, whose density profile is defined by the Lane-Emden equa-

DSph	$\text{Log } \rho_0$ [ $M_\odot/\text{pc}^3$ ]	$d_0$ [kpc]	lower bound on $m$
Triangulum II	0.3	30	127 eV
Segue 1	-0.4	32	100 eV
Leo T	-0.6	417	26 eV
Reticulum II	-0.8	32	89 eV
Ursa Major I	-0.8	106	49 eV
Coma Berenices	-0.8	44	76 eV
Sculptor	-0.8	86	54 eV
Fornax	-1.1	147	38 eV
Ursa Major II	-1.2	32	80 eV
Leo I	-1.3	254	27 eV
Canes Venatici II	-1.4	151	34 eV
Hercules	-1.4	132	37 eV
Pisces II	-1.5	180	30 eV
Leo IV	-1.7	158	31 eV
Leo II	-1.7	233	25 eV
Draco II	-1.9	20	82 eV
Sextans	-2.	86	38 eV
Canes Venatici I	-2.2	224	22 eV
Carina	-2.2	106	33 eV
Bootes I	-2.4	66	39 eV
Leo V	-2.6	178	22 eV
Draco	-2.7	76	33 eV
Hydra II	-3.1	134	22 eV
Segue 2	-3.2	35	43 eV

TABLE I. Estimated lower bound on the fermionic DM mass  $m$  from a number of dwarf spheroidal galaxies, adopting the central densities as determined in [38].

tion. We have performed a fit of the stellar velocity dispersion predicted by the gravitational potential generated by such DM halo, versus the observed stellar dispersion velocity and density profile of the Willman I, Segue I and Leo II galaxies. In our analysis, differently from recent works on the subject, we have not assumed that luminous matter traces the DM distribution, thus we have considered the DM core radius and surface density as free parameters. Moreover, we have taken into account the effect of the unknown anisotropy of the stellar velocity dispersion and marginalized over it.

As we have shown, the nuisance due to the stellar velocity anisotropy  $\beta$  seriously hampers the possibility to constrain completely the DM halo parameters. In practice, one finds equally acceptable halos of very small sizes and negative  $\beta$  (where the total DM halo mass is determined) or very large sizes  $\sim \text{few kpc}$  and anisotropy near 1 (in which case the inner DM spatial density is determined). This latter scenario effectively corresponds to low phase-space densities, and thus no sensible lower bound on  $m$  can be given from stellar kinematical data alone. This situation is likely to persist even in the future,

until a way to measure the velocity anisotropy in dwarfs spheroidals will be available (see e.g. [39]) although this appears currently quite unconceivable.

Such multi-kpc halos are in any case unrealistic and a rationale to rule them out is provided [19] by the fact that very large halos of known density correspond to large total halo mass, which makes their time of orbital decay due to dynamical friction in the Galactic DM halo, formula (15), too small. Therefore, dynamical friction can be used to effectively limit the halo size and the interplay with the quantum bound on phase-space density leads finally to a lower bound on the fermionic DM mass  $m$ .

As it turns out from the analysis that we presented, at present the most restrictive bound stems from the study of the Willman I and Segue I galaxies. Our results are put together in Figure 1, where only the interplay between the fit to stellar data and the constraint from dynamical friction leads to a robust lower bound of  $m \gtrsim 100$  eV. Thus, one is led to reopen the case for sub-keV fermionic DM, like sterile neutrinos of mass down to 100 eV.

For these two small dwarf galaxies driving the bound, the resulting DM halo can reach sizes of  $\sim 1$  kpc, much larger than their stellar components. This does not mean that all the dwarf spheroidal galaxies shall have such enhanced halos; this could likely hold only for these smallest objects that approach the fermionic degenerate regime.

As far as DM indirect detection is concerned, we note that the expected flux from DM annihilation (so called  $J$ -factor) is enhanced in the limiting case of the extended halo sizes considered here, compensating the naturally low flux characteristic of cored halos. At the same time, the dynamical friction upper bound on the halo sizes will slightly reduce the maximal expected  $J$ -factor in cored halos, with respect to the analysis of e.g. [38].

Clearly, DM masses  $m = 100$  eV are at odds with bounds derived from the effect of warm dark matter on structure formation (e.g. Lyman- $\alpha$ ) that typically forbid masses below few keV, see e.g. [30], by limiting their free streaming length. Therefore, for this scenario to be realistic, the spectrum of such DM candidates should be much colder than usual (see e.g. [40]). This can be realized in models with production via decay as e.g. in [24, 41], or for instance in models in which DM at decoupling is overabundant and then subject to dilution by decays of other species, along the lines of e.g. [42, 43].

More theoretically, in order to attain the fermionic degeneracy that we have tested, it is also necessary that either the maximum of the primordial phase-space density saturates the occupation limit (A5) as it happens e.g. in relativistic decoupling, or alternatively that DM is subject to some form of dissipation or interaction, so that the phase-space density might grow during collapse. Indeed, a very interesting (and outstanding) issue is that of which collapse mechanism and time scales could lead to degenerate fermionic halos. While the free energy and entropy budget have been shown to be favorable [21, 44, 45], an assessment of the dynamics and relaxation times is still beyond reach see [46, 47].

On the observational side, it is worth commenting that while the DSph galaxies are the smallest and most DM dominated astrophysical objects, with a number of new dwarfs being currently discovered by present surveys, the possibility of using other types of galaxies for setting a bound on  $m$  from degeneracy is also of interest. Recently, cored halo mass modelings of Disk Dwarf galaxies from the Little Things survey have been performed, see [48]. Although the rotation curve decomposition is affected by uncertainty in the asymmetric drift gas contribution, due to their disk structure they are not subject to the dramatic anisotropy nuisance parameter of dwarf spheroidals and could potentially lead to a better bound on the DM mass  $m$ .

## ACKNOWLEDGMENTS

We thank Neven Bilić, Kathy Karukes, Paolo Salucci and Piero Ullio for useful discussions. F.N. was partially supported by the H2020 CSA Twinning project No. 692194 “RBI-T-WINNING”.

## Appendix A: Self-gravitating fermionic gas

We briefly review in this appendix the analysis of the equilibrium distribution of a self-gravitating gas of neutral fermions. We describe first the limiting case of complete degeneration and then we recall the Thomas-Fermi treatment which allows to describe the transition to partially or non-degenerate case.

*a. Stability conditions for the DM halo.* If we have large number of DM particles, we can assume they move in a spherically symmetric mean-field gravitational potential  $\phi(r)$  which satisfies the Poisson’s equation:

$$\begin{aligned} \frac{d\phi}{dr} &= \frac{GM}{r^2} \\ \frac{dM}{dr} &= 4\pi r^2 \rho, \end{aligned} \quad (\text{A1})$$

where  $M(r)$  is the mass enclosed within the radius  $r$ ,  $G$  is the Newton’s constant and  $\rho(r)$  is the matter density. For non relativistic particles, the density can be expressed as:

$$\rho = m \int dp \, 4\pi p^2 f(p), \quad (\text{A2})$$

where  $m$  is the particle mass and we assumed that DM distribution function  $f(p)$  is isotropic. The dynamical stability of the system is expressed by the Jeans equation:

$$\frac{d}{dr}(\rho \sigma_{\text{DM}}^2) = -\rho \frac{d\phi}{dr}, \quad (\text{A3})$$

where the DM velocity dispersion  $\sigma_{\text{DM}}^2$  is given by:

$$\sigma_{\text{DM}}^2 = \frac{1}{3} \frac{\int dp \, p^4 / m^2 f(p)}{\int dp \, p^2 f(p)} \quad (\text{A4})$$

If DM is composed by fermions, the distribution function  $f(p)$  has an upper limit:

$$f(p) \leq \frac{g}{(2\pi)^3}, \quad (\text{A5})$$

where we use  $\hbar = 1$  and  $g$  represents the number of internal (spin) degrees of freedom. This automatically implies that a lower limit exists for the velocity dispersion

$$\sigma_{\text{DM}}^2 \geq \sigma_{\text{DM,min}}^2 = \frac{1}{5} \left( \frac{6\pi^2 \rho}{g m^4} \right)^{2/3} \quad (\text{A6})$$

of a fermionic system of fixed density.

*b. The strong degeneracy limit.* In the strong degeneracy regime, the states with energy below the Fermi energy  $\varepsilon$  are fully occupied, i.e. the distribution function  $f(p)$  has the form:

$$f(p) = \begin{cases} \frac{g}{(2\pi)^3} & p < p_F \\ 0 & p > p_F \end{cases} \quad (\text{A7})$$

where  $p_F = \sqrt{2m\varepsilon}$  is the Fermi momentum. In this assumption, one obtains the expressions:

$$\begin{aligned} \rho &= K \varepsilon^{3/2} \\ \sigma_{\text{DM}}^2 &= K' \varepsilon, \end{aligned} \quad (\text{A8})$$

where  $K = \sqrt{2} g m^{5/2} / (3\pi^2)$  and  $K' = 2/(5m)$ , that permit to recast Eqs. (A1,A3) in the form

$$\frac{1}{r^2} \frac{d}{dr} \left[ r^2 \frac{d\varepsilon(r)}{dr} \right] = -4\pi G m K \varepsilon(r)^{3/2}. \quad (\text{A9})$$

The above equation has to be integrated with the condition  $d\varepsilon(0)/dr = 0$  ensuring that the gravitational acceleration is zero at the galaxy center. By defining

$$\xi \equiv r/\tilde{r}, \quad (\text{A10})$$

where the scale radius  $\tilde{r}$  is given by

$$\tilde{r} \equiv \frac{1}{\sqrt{4\pi G m K \varepsilon_0^{1/2}}} = \frac{1}{\sqrt{4\pi G m K^{2/3} \rho_0^{1/3}}}, \quad (\text{A11})$$

and by using the function  $\theta(\xi)$  defined as

$$\theta(\xi) \equiv \frac{\varepsilon(\xi)}{\varepsilon_0} = \left[ \frac{\rho(\xi)}{\rho_0} \right]^{2/3}, \quad (\text{A12})$$

where  $\varepsilon_0$  ( $\rho_0$ ) is the central value of the Fermi energy (density), eq. (A9) can be rewritten in the form

$$\frac{1}{\xi^2} \frac{d}{d\xi} \left[ \xi^2 \frac{d\theta(\xi)}{d\xi} \right] = -\theta(\xi)^{3/2}, \quad (\text{A13})$$

which is the well-know Lane-Emden equation.

Eqs. (A12) and (A13) show that the profiles of degenerate Fermionic DM halos are universal and depend

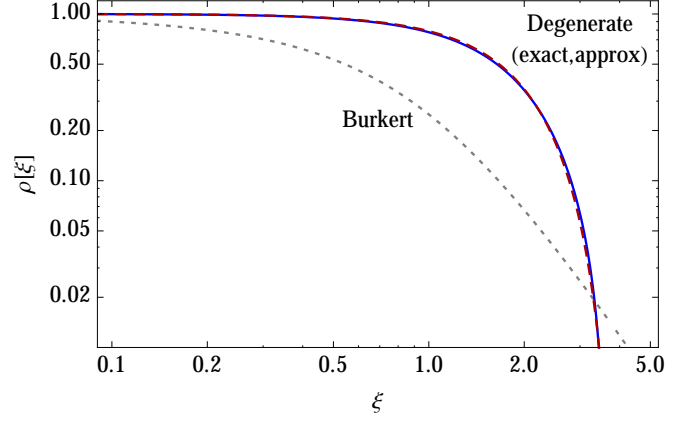


FIG. 9. Density profiles for the DM halos. Solid: the solution of the Lane-Emden equation for degenerate fermions. Dashed: its approximation adopted in the text (A14). Dotted: the Burkert density profile for comparison.

only on the assumed central density  $\rho_0$  and DM particle mass  $m$ . The mass distribution crucially differs from the usually adopted cusped or cored profiles. A sharp transition exists from an internal core with high and quite uniform density to an external region devoid of DM. For our purposes, the density profile of degenerate fermionic DM halos can be well approximated by

$$\rho(\xi) = \rho_0 \cos^3 \left[ \frac{\pi}{8} \xi \right] \quad (\text{A14})$$

for  $0 \leq \xi \leq 3.65$ , and  $\rho(\xi) = 0$  elsewhere. This is depicted in Fig. 9.

We define the halo radius by the condition  $\rho(\xi_h) = \rho_0/4$  that gives  $\xi_h = 2.26$  corresponding to:

$$\begin{aligned} R_h &\equiv \xi_h \tilde{r} = \\ &= 42.4 \text{ pc} \left( \frac{g}{2} \right)^{-1/3} \left( \frac{m}{1 \text{ keV}} \right)^{-4/3} \left( \frac{\rho_0}{\text{M}_\odot \text{ pc}^{-3}} \right)^{-1/6}. \end{aligned} \quad (\text{A15})$$

By using the above expression, we rewrite eq. (A14) in the form:

$$\rho(r) = \rho_0 \cos^3 \left[ \frac{25}{88} \pi \frac{r}{R_h} \right], \quad (\text{A16})$$

where we used the approximate equality  $\xi_h/8 \simeq 25/88$ .

*c. The Thomas-Fermi model for fermionic DM.* A self consistent description of isothermal fermionic DM halos with an arbitrary level of degeneracy can be obtained by using a Thomas-Fermi approach, see [20, 22]. We assume that DM particles follow a Fermi-Dirac distribution

$$f_{\text{FD}}(p; T, \mu) = \frac{g}{(2\pi)^3} \frac{1}{\exp[(E - \mu)/T] + 1}, \quad (\text{A17})$$

where  $E = p^2/(2m)$  is the single-particle kinetic energy,  $T$  is the temperature and  $\mu$  is the chemical potential. In



the above, the density can be expressed as:

$$\rho = \frac{g(2T)^{3/2}m^{5/2}}{6\pi^2} I_2(\nu) \quad (\text{A18})$$

where

$$I_2(\nu) \equiv 3 \int_0^\infty dy \frac{y^2}{\exp(y^2 - \nu) + 1} \quad (\text{A19})$$

and  $\nu \equiv \mu/T$  is a degeneracy parameter.

If one assumes that the temperature is constant,  $T(r) \equiv \tilde{T}$ , and that the chemical potential at each given radius is related to the gravitational potential  $\phi(r)$  by

$$\mu(r) = \tilde{\mu} - m\phi(r) \quad (\text{A20})$$

where  $\tilde{\mu}$  is a constant, then the Jeans equation (A3) is automatically fulfilled and Eqs. (A1), (A2) can be recast in the form

$$\frac{1}{r^2} \frac{d}{dr} \left[ r^2 \frac{d\mu(r)}{dr} \right] = -4\pi G m \rho(r), \quad (\text{A21})$$

again to be integrated with the condition  $d\mu(0)/dr = 0$  for zero gravitational acceleration at the galaxy center.

*d. The non degenerate case.* The Thomas-Fermi approach just described has the advantage of automatically implementing the upper limit (A5) imposed by the Pauli exclusion principle; it can thus describe the transition between classical and degenerate structures, in a continuous way. By using this approach, one is able to see that when  $R_h$  is 2-3 times larger than the minimal value in eq. (A15) the fermionic nature of DM particles can be neglected, i.e. the resulting structures are essentially indistinguishable from cored isothermal halos obtained by

assuming Maxwell-Boltzmann statics and arbitrary values of the particle mass  $m$ .

The approach considered does not allow, however, to unambiguously predict the halo properties in the non degenerate case. Indeed, in the classical regime (i.e. for  $\nu \ll 1$ ) one has  $I_2(\nu) \simeq \exp(\nu)$ , differently from the strongly degenerate case in which  $I_2(\nu) \simeq \nu^{3/2}$ . Thus, the r.h.s. of eq. (A21) depends both on the temperature and the chemical potential. One obtains then a family of solutions depending on these two free parameters, the temperature  $\tilde{T}$  and the assumed chemical potential  $\mu_0$  (or, equivalently, the assumed density  $\rho_0$ ) at the center of the system. Moreover, a temperature profile, typically constant, has to be assumed in the Thomas-Fermi approach in order to solve eq. (A3). In a more realistic scenario, in which the temperature may vary along the galactic structure,  $\tilde{T}$  could be regarded as the central temperature; the predictions obtained in the degenerate or semi-degenerate regimes are thus valid in the central core where temperature variations can be neglected, while the properties of the external region depend on the radial temperature profile. As it is natural to expect, basing on sole theoretical grounds it is thus impossible to predict the mass distribution in regions of non degeneration.

For this reason in the text, where we refer to non-degenerate halos, we model them by using the observationally supported Burkert profile:

$$\rho_{\text{Bur}}(r) = \frac{\rho_0}{(1+x)(1+x^2)}, \quad x = r/R_h. \quad (\text{A22})$$

We require that the central density  $\rho_0$  and core radius  $R_h$  are consistent with the assumption of non degenerate structure composed by fermions with mass  $m$  and  $g$  spin degrees of freedom, i.e. for each assumed value of  $\rho_0$ , the halo radius  $R_h$  is required to be a factor  $\sim 2$  larger than the degenerate limit expressed by Eq. (A15).

- 
- [1] David H. Weinberg, James S. Bullock, Fabio Governato, Rachel Kuzio de Naray, and Annika H. G. Peter. Cold dark matter: controversies on small scales. *Proc. Nat. Acad. Sci.*, 112:12249–12255, 2014.
  - [2] Ricardo A. Flores and Joel R. Primack. Observational and theoretical constraints on singular dark matter halos. *Astrophys. J.*, 427:L1–4, 1994.
  - [3] Julio F. Navarro, Carlos S. Frenk, and Simon D. M. White. The Structure of cold dark matter halos. *Astrophys. J.*, 462:563–575, 1996.
  - [4] Julio F. Navarro, Carlos S. Frenk, and Simon D. M. White. A Universal density profile from hierarchical clustering. *Astrophys. J.*, 490:493–508, 1997.
  - [5] B. Moore. Evidence against dissipationless dark matter from observations of galaxy haloes. *Nature*, 370:629, 1994.
  - [6] Ben Moore, Thomas R. Quinn, Fabio Governato, Joachim Stadel, and George Lake. Cold collapse and the core catastrophe. *Mon. Not. Roy. Astron. Soc.*, 310:1147–1152, 1999.
  - [7] Paolo Salucci and Andreas Burkert. Dark matter scaling relations. *Astrophys. J.*, 537:L9–L12, 2000.
  - [8] B. Moore, S. Ghigna, F. Governato, G. Lake, Thomas R. Quinn, J. Stadel, and P. Tozzi. Dark matter substructure within galactic halos. *Astrophys. J.*, 524:L19–L22, 1999.
  - [9] Anatoly A. Klypin, Andrey V. Kravtsov, Octavio Valenzuela, and Francisco Prada. Where are the missing Galactic satellites? *Astrophys. J.*, 522:82–92, 1999.
  - [10] Julio F. Navarro, Vincent R. Eke, and Carlos S. Frenk. The cores of dwarf galaxy halos. *Mon. Not. Roy. Astron. Soc.*, 283:L72–L78, 1996.
  - [11] Fabio Governato et al. At the heart of the matter: the origin of bulgeless dwarf galaxies and Dark Matter cores. *Nature*, 463:203–206, 2010.
  - [12] F. Governato, A. Zolotov, A. Pontzen, C. Christensen, S. H. Oh, A. M. Brooks, T. Quinn, S. Shen, and J. Wadsley. Cuspy No More: How Outflows Affect the Central Dark Matter and Baryon Distribution in Lambda CDM

- Galaxies. *Mon. Not. Roy. Astron. Soc.*, 422:1231–1240, 2012.
- [13] Andrew Pontzen and Fabio Governato. How supernova feedback turns dark matter cusps into cores. *Mon. Not. Roy. Astron. Soc.*, 421:3464, 2012.
- [14] Pedro Colin, Vladimir Avila-Reese, and Octavio Valenzuela. Substructure and halo density profiles in a warm dark matter cosmology. *Astrophys. J.*, 542:622–630, 2000.
- [15] Paul Bode, Jeremiah P. Ostriker, and Neil Turok. Halo formation in warm dark matter models. *Astrophys. J.*, 556:93–107, 2001.
- [16] Vladimir Avila-Reese, Pefro Colin, Octavio Valenzuela, Elena D’Onghia, and Claudio Firmani. Formation and structure of halos in a warm dark matter cosmology. *Astrophys. J.*, 559:516–530, 2001.
- [17] S. Tremaine and J. E. Gunn. Dynamical Role of Light Neutral Leptons in Cosmology. *Phys. Rev. Lett.*, 42:407–410, 1979.
- [18] Julianne J. Dalcanton and Craig J. Hogan. Halo cores and phase space densities: Observational constraints on dark matter physics and structure formation. *Astrophys. J.*, 561:35–45, 2001.
- [19] O. E. Gerhard and D. N. Spergel. Dwarf spheroidal galaxies and the mass of the neutrino. *The Astrophysical Journal Letters*, 389:L9–L11, April 1992.
- [20] Neven Bilic, Gary B. Tupper, and Raoul D. Viollier. Unified description of dark matter at the center and in the halo of the Galaxy. 2001.
- [21] Pierre-Henri Chavanis. Phase transitions in self-gravitating systems: Self-gravitating fermions and hard spheres models. *Phys. Rev.*, E65:056123, 2002.
- [22] H. J. de Vega, P. Salucci, and N. G. Sanchez. Observational rotation curves and density profiles versus the Thomas-Fermi galaxy structure theory. *Mon. Not. Roy. Astron. Soc.*, 442(3):2717–2727, 2014.
- [23] Alexey Boyarsky, Oleg Ruchayskiy, and Dmytro Iakubovskiy. A Lower bound on the mass of Dark Matter particles. *JCAP*, 0903:005, 2009.
- [24] Valerie Domcke and Alfredo Urbano. Dwarf spheroidal galaxies as degenerate gas of free fermions. *JCAP*, 1501(01):002, 2015.
- [25] F. Donato, G. Gentile, P. Salucci, C. Frigerio Martins, M. I. Wilkinson, G. Gilmore, E. K. Grebel, A. Koch, and R. Wyse. A constant dark matter halo surface density in galaxies. *Mon. Not. Roy. Astron. Soc.*, 397:1169–1176, 2009.
- [26] Paolo Salucci, Mark I. Wilkinson, Matthew G. Walker, Gerard F. Gilmore, Eva K. Grebel, Andreas Koch, Christiane Frigerio Martins, and Rosemary F. G. Wyse. Dwarf spheroidal galaxy kinematics and spiral galaxy scaling laws. *Mon. Not. Roy. Astron. Soc.*, 420:2034, 2012.
- [27] Beth Willman, Marla Geha, Jay Strader, Louis E. Strigari, Joshua D. Simon, Evan Kirby, and Alex Warres. Willman 1 - a probable dwarf galaxy with an irregular kinematic distribution. *Astron. J.*, 142:128, 2011.
- [28] Joshua D. Simon et al. A Complete Spectroscopic Survey of the Milky Way Satellite Segue 1: The Darkest Galaxy. *Astrophys. J.*, 733:46, 2011.
- [29] J. Binney and S. Tremaine. *Galactic Dynamics*, 2<sup>nd</sup> edition. Princeton University Press, 2008.
- [30] Vid Iršič et al. New Constraints on the free-streaming of warm dark matter from intermediate and small scale Lyman- $\alpha$  forest data. 2017.
- [31] Joe Wolf, Gregory D. Martinez, James S. Bullock, Manoj Kaplinghat, Marla Geha, Ricardo R. Munoz, Joshua D. Simon, and Frank F. Avedo. Accurate Masses for Dispersion-supported Galaxies. *Mon. Not. Roy. Astron. Soc.*, 406:1220, 2010.
- [32] M. Walker. *Dark Matter in the Galactic Dwarf Spheroidal Satellites*, page 1039. 2013.
- [33] Matthew G. Walker, Mario Mateo, Edward W. Olshewski, Oleg Y. Gnedin, Xiao Wang, Bodhisattva Sen, and Michael Woodroffe. Velocity Dispersion Profiles of Seven Dwarf Spheroidal Galaxies. *Astrophys. J.*, 667:L53, 2007.
- [34] Piero Ullio and Mauro Valli. A critical reassessment of particle Dark Matter limits from dwarf satellites. *JCAP*, 1607(07):025, 2016.
- [35] A. Just, F. M. Khan, P. Berczik, A. Ernst, and R. Spurzem. Dynamical friction of massive objects in galactic centres. *Mon. Not. Roy. Astron. Soc.*, 411:653–674, February 2011.
- [36] Justin I. Read, Tobias Goerdt, Ben Moore, A. P. Pontzen, Joachim Stadel, and George Lake. Dynamical friction in constant density cores: A failure of the Chandrasekhar formula. *Mon. Not. Roy. Astron. Soc.*, 373:1451–1460, 2006.
- [37] Fabrizio Nesti and Paolo Salucci. The Dark Matter halo of the Milky Way, AD 2013. *JCAP*, 1307:016, 2013.
- [38] Kohei Hayashi, Koji Ichikawa, Shigeki Matsumoto, Masahiro Ibe, Miho N. Ishigaki, and Hajime Sugai. Dark matter annihilation and decay from non-spherical dark halos in galactic dwarf satellites. *Mon. Not. Roy. Astron. Soc.*, 461(3):2914–2928, 2016.
- [39] J. I. Read and P. Steger. How to break the density-anisotropy degeneracy in spherical stellar systems. *ArXiv e-prints*, January 2017.
- [40] M. Drewes et al. A White Paper on keV Sterile Neutrino Dark Matter. *JCAP*, 1701(01):025, 2017.
- [41] Kalliopi Petraki and Alexander Kusenko. Dark-matter sterile neutrinos in models with a gauge singlet in the Higgs sector. *Phys. Rev.*, D77:065014, 2008.
- [42] F. Bezrukov, H. Hettmansperger, and M. Lindner. keV sterile neutrino Dark Matter in gauge extensions of the Standard Model. *Phys. Rev.*, D81:085032, 2010.
- [43] Miha Nemevsek, Goran Senjanovic, and Yue Zhang. Warm Dark Matter in Low Scale Left-Right Theory. *JCAP*, 1207:006, 2012.
- [44] Peter Hertel, Heide Narnhofer, and Walter E. Thirring. Thermodynamic functions for fermions with gravostatic and electrostatic interactions. *Commun. Math. Phys.*, 28:159–176, 1972.
- [45] Neven Bilic and Raoul D. Viollier. Gravitational phase transition of heavy neutrino matter. *Phys. Lett.*, B408:75–80, 1997.
- [46] Pierre-Henri Chavanis, Mohammed Lemou, and Florian Méhats. Models of dark matter halos based on statistical mechanics: The classical King model. *Phys. Rev.*, D91(6):063531, 2015.
- [47] Alessandro Campa, Thierry Dauxois, and Stefano Ruffo. Statistical mechanics and dynamics of solvable models with long-range interactions. *Phys. Rept.*, 480(3-6):57–159, 2009.
- [48] E. V. Karukes and P. Salucci. The universal rotation curve of dwarf disk galaxies. *Mon. Not. Roy. Astron. Soc.*, 2016.